

Evaluation of coupling parameters of EMC filter components by using equivalent emission sources

Sanaa Zangui, Kévin Berger, Benjamin Vincent, Ronan Perrussel, Edith Clavel, Christian Vollaire, Carlos Sartori, Laurent Krähenbühl

► To cite this version:

Sanaa Zangui, Kévin Berger, Benjamin Vincent, Ronan Perrussel, Edith Clavel, et al.. Evaluation of coupling parameters of EMC filter components by using equivalent emission sources. V. C. Silva. MOMAG, Aug 2010, Vitória, Brazil. Proceeding of the 14^o Simpósio Brasileiro de Microondas e Optoeletrônica e o 9^o Congresso Brasileiro de Eletromagnetismo, pp.CD, 2010. <hal-00502220>

HAL Id: hal-00502220

<https://hal.archives-ouvertes.fr/hal-00502220>

Submitted on 13 Jul 2010

HAL is a multi-disciplinary open access archive for the deposit and dissemination of scientific research documents, whether they are published or not. The documents may come from teaching and research institutions in France or abroad, or from public or private research centers.

L'archive ouverte pluridisciplinaire **HAL**, est destinée au dépôt et à la diffusion de documents scientifiques de niveau recherche, publiés ou non, émanant des établissements d'enseignement et de recherche français ou étrangers, des laboratoires publics ou privés.

EVALUATION OF COUPLING PARAMETERS OF EMC FILTER COMPONENTS BY USING EQUIVALENT EMISSION SOURCES

S. Zangui*, K. Berger *, B. Vincent*, R. Perrussel*, E. Clavel**, C. Vollaire*, C. Sartori***, L.Krähenbühl*

(*) : Laboratoire Ampère – UMR CNRS 5005, Ecole Centrale de Lyon, 36 Avenue Guy de Collongue, 69130 Ecully, sanaa.zangui@ec-lyon.fr, christian.vollaire@ec-lyon.fr, benjamin.vincent@ec-lyon.fr, ronan.perrussel@ec-lyon.fr, Laurent.Krahenbuhl@ec-lyon.fr

(**) : Laboratoire G2Elab – UMR CNRS 5269, Site principal campus ENSE3 bat D 961, rue Houille Blanche BP 46, 38402 St Martin d'Hères Cedex, edith.clavel@g2elab.grenoble-inp.fr

(***) : Escola Politécnica da Universidade de São Paulo LMAG/PEA/EPUSP, Av.Prof.Luciano Gualberto, TRav.3.-CEP- 05508-970- São Paulo, SP-Brasil, Sartori@pea.usp.br

Abstract—EMC filters are increasingly integrated into power applications. To improve the filter performance it is important to model the electromagnetic interference between components to optimize their positions. In this paper, a method is proposed to construct the equivalent model of the filter components. The proposed method is based on the multipolar expansion by representing the radiation emission of generic structures in a spherical reference (r, θ, φ) . These models of the sources will be used to compute the mutual inductance between the components according to their geometric placement.

I. INTRODUCTION

EMC filters are designed to improve the electromagnetic compatibility and the immunity level of electric and electronic systems, in particular the aspects concerning power quality and electromagnetic signature. For this reason the behavior of these filters has to be studied. Concerning these studies, the evaluation of the electrical parameters of the filter components assumes an important role. Basically, there are two types of parasitic parameters: the self-parasitic of the filter components and the mutual parasitic that reflect the coupling between components. Fig.1 represents the electric model of an EMC filter « Π » consisting of two capacitors C_{y1} and C_{y2} , and an inductance L_{DM} . This model includes the self-parasitic of the filter components and the inductive coupling between components [1]. The capacitive effects are not considered. Due to the significant current values related the filter when compared with the voltage one, this simplified model is assumed.

In Fig.1 the following notations are used:

- ESL, ESR, C: The self-parasitic parameters, inductance, resistance, and the capacitance,
- L_{DM} , EPC, EPR: The inductance, and the related self-parasitic capacitance and the resistance,
- M_1 and M_2 : Mutual inductances between L_{DM} and the self-parasitic inductances ESL_1 and ESL_2 ,
- M_3 : Mutual inductance between the self-parasitic inductances ESL_1 and ESL_2 ,
- M_4 : Coupling inductance between L_{DM} and the PCB tracks.

As Fig.2 shows, these parasitic parameters can affect the EMC filter performances. This figure was withdraw from [2], and it presents three curves: the first one called “base” represents the filter behavior before implementing the electromagnetic interference reduction and the filter performance improvement, the second “Minimized coupling” was obtained by optimizing the location of the components to reduce the coupling between filter components, and the third curve “Minimized coupling + ESL cancellation” represents the filter behavior after reducing the mutual parasitic and the effect of the equivalent serial inductance ESL. The part A calls the attention to the differences between the first curve “base” and the second curve “Minimized coupling”, in particular to the first resonance frequency that matches the coupling effect of the filter components (mutual inductances). In a similar way, the part B stress the difference between the curves “base” and the “Minimized coupling + ESL cancellation”, and the impact of the self-parasitic components.

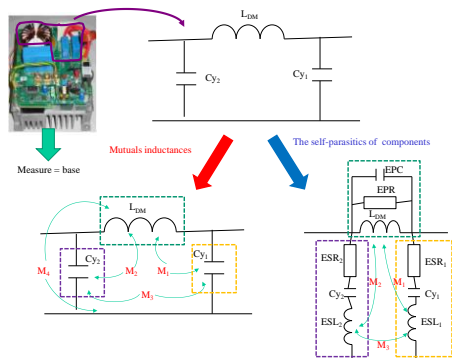


Fig.1 – Filter with parasitic coupling and the self-parasitic.

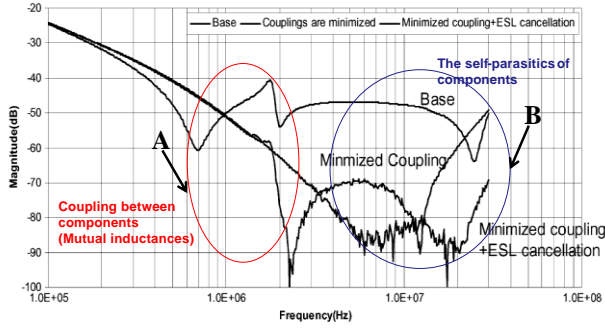


Fig.2 – Effect of parasitic parameters, extract from [2].

Thus, in a converter including passive and active components, the component mutual parasitic modeling can be considered as a fundamental problem.

Nevertheless, it should be mentioned that, currently, there is not a suitable methodology that takes into account the near-field coupling between components when an accurate evaluation of filter performances is required.

The objective of this work is to propose a methodology suitable for obtain models that could represent the radiated field of the filter components, at a wide range of frequencies, useful to evaluating the filter performance. In particular, these models will be applied to determine the coupling effects between the filter components, basically the mutual inductance, considering the influence of parameters, such as the distance between components etc.

As the distance between components is much smaller than the wavelength related to the frequencies of power electronic applications, usually ($f < 100\text{MHz}$), a quasi static approach can be considered. It is the case of a magnetic source, in which the capacitive effects are negligible.

The method proposed to determine the equivalent radiated field model of the filter components by applying the multipolar expansion. It can be used to represent the radiation of generic structures (coils, capacities, tracks...), and the spherical coordinates (r, θ, φ) is considered in this work.

Basically, this method will be used to compute the coupling effects between discrete filter components (capacitors, resistances and inductances). To simulate the whole configuration, the coupling between tracks should also be taken into account. The PEEC method is used to determine the inductive and resistive effects (R, L, M). On the other hand, for the parasitic capacitors evaluations, the MoM (Moments method) and the Fast Multipolar Method FMM are used [3]. For the tracking connection, the equivalent sources corresponding to discrete components can be integrated. This can simplify the model and improve the memory allocation.

II. MULTIPOLAR EXPANSION

A. Definition

The multipolar expansion can be used to represent the electromagnetic fields in 3D, assuming that the field is computed outside the sphere of radius r that contains the equivalent source (Fig.3).

The multipolar expansion of the electric and magnetic fields is deduced from the solution of the magnetic vector potential A_r and the electric vector potential F_r given by [4]:

$$\mathbf{F}_r(r, \theta, \varphi) = \sum_{n=1}^{\infty} \sum_{m=-n}^n Q_{nm}^{(cf)} \hat{B}_n^{(cf)}(kr) P_n^m(\cos\theta) e^{jm\varphi} \quad (1)$$

$$\mathbf{A}_r(r, \theta, \varphi) = \sum_{n=1}^{\infty} \sum_{m=-n}^n Q_{nm}^{(ca)} \hat{B}_n^{(ca)}(kr) P_n^m(\cos\theta) e^{jm\varphi} \quad (2)$$

The notation (cf) and (ca) determine the type of the function $\hat{B}_n(kr)$. For example, for a progressive wave propagating along $(+r)$, when $c = 4$, and $\hat{B}_n(kr) = \hat{H}_n^{(2)}(kr)$, it will correspond to the spherical Hankel functions [4].

If these functions are chosen, the expressions of the electric field \mathbf{E} and the magnetic field \mathbf{H} can be represented by the following expressions [4]:

$$\mathbf{E}(r, \theta, \varphi) = \sum_{n=1}^{\infty} \sum_{m=-n}^n Q_{1nm}^{(4)} F_{1nm}^{(4)}(r, \theta, \varphi) + Q_{2nm}^{(4)} F_{2nm}^{(4)}(r, \theta, \varphi) \quad (3)$$

$$\mathbf{H}(r, \theta, \varphi) = \frac{j}{\eta} \sum_{n=1}^{\infty} \sum_{m=-n}^n Q_{2nm}^{(4)} F_{1nm}^{(4)}(r, \theta, \varphi) + Q_{1nm}^{(4)} F_{2nm}^{(4)}(r, \theta, \varphi) \quad (4)$$

with $\eta = \sqrt{\frac{\mu}{\epsilon}}$ the intrinsic impedance of the considered environment.

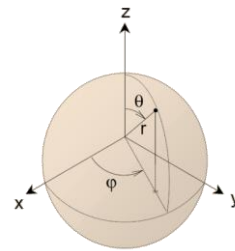


Fig.3 – References adopted in the field computation

The coefficients $Q_{1nm}^{(4)}$ describe the strength of the transverse-electric (TE) components of the radiated field, while coefficients $Q_{2nm}^{(4)}$ describe the strength of the transverse-magnetic (TM) components. These coefficients are the parameters to be identified to characterize the equivalent model of the radiated field component.

$F_{1nm}^{(4)}$ and $F_{2nm}^{(4)}$ are the vector's spherical harmonics which are a solution of Maxwell's equations in free space,

excluding the sphere that involves the sources. To compute the vector spherical harmonics, the solution of the scalar Helmholtz equation is used:

$$F_{1nm}^{(4)} = \vec{\nabla} \times (\Psi_{nm}^{(4)} r) \quad F_{2nm}^{(4)} = \frac{1}{k} \vec{\nabla} \times F_{1nm}^{(4)} \quad (5)$$

The solution of the Helmholtz equation is then expressed as follows:

$$\Psi_{nm}^{(4)}(r, \theta, \varphi) = \frac{j}{\sqrt{n(n+1)}} Q_{snm}^{(4)} b_n^{(4)}(kr) Y_{nm}(\theta, \varphi) \quad (6)$$

where Y_{nm} are the normalized spherical harmonics

$$Y_{nm}(\theta, \varphi) = \sqrt{\frac{2n+1(n-m)!}{4\pi(n+m)!}} P_n^m(\cos\theta) e^{jm\varphi} \quad (7)$$

In the aforementioned equations:

n : degree,

m : azimuthal order,

k : the phase constant,

r : distance from the center of the coordinate system,

b_n : The Bessel functions,

P_n^m : The Legendre associated functions.

B. Application

It should be mentioned that, in order to represent the component radiated field in spherical harmonics, it is necessary to compute the coefficients of the decomposition Q_{nm} . In the case of a magnetic source in the near-field, the coefficients associated to the magnetic transverse modes are negligible because the electric field is considered very low compared to the magnetic field. These coefficients are functions of $\mathbf{H}(r, \theta, \varphi)$, and can be obtained by applying [4]:

$$\mathbf{H} = \frac{j}{\eta} \sum_{n=1}^{\infty} \sum_{m=-n}^n \frac{(2n-1)!!}{(kr)^{n+2}} N_n^m e^{jm\varphi} Q_{nm}^{(4)} \begin{cases} n(n+1)P_n^m(\cos\theta)\hat{a}_r \\ -n \frac{dP_n^m(\cos\theta)}{d\theta} \hat{a}_\theta \\ -n \frac{jmP_n^m(\cos\theta)}{\sin\theta} \hat{a}_\varphi \end{cases} \quad (8)$$

with

$$N_n^m = j \sqrt{\frac{2n+1}{4\pi} \frac{(n-m)!}{n(n+1)(n+m)!}} \quad (9)$$

Depending on the complexity of the object to model, we can calculate the radiated \mathbf{H} -field by using a 3D model or by performing experimental measurements [5]. Some components of the multipolar expansion can be directly measured using novel magnetic induction sensors, for example, the sensors based on the standard CISPR16-1 coils [6].

III. MEASUREMENT APPROACH USED TO IDENTIFY THE COMPONENTS OF THE MULTIPOLAR EXPANSION

The approach used to identify the components of the multipolar expansion consists in measuring the magnetic flux coupled with large coils placed around the device in order to achieve a special integration. The measurement principle is similar to a special filtering: according to the coil shape, each sensor is sensitive to one specific component of the multipolar expansion [5]. The prototype is shown in Fig.4:

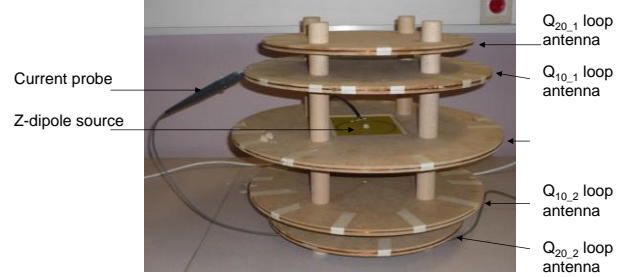


Fig.4 – The prototype to identify the terms of the multipolar expansion [5].

The basic principle is to measure the magnetic flux through different coils in short circuit mode on the measurement sphere S_M (radius r_M) around the device. The flux across the surface delimited by the set of coils is expressed by:

$$\begin{aligned} \mathbf{Flux}_{nm} &= \iint_{\text{coil surface}} (\mu \cdot \mathbf{H}(r_M, \theta, \varphi) \cdot \mathbf{n}) ds \\ &= \frac{\mu_0}{4\pi} \frac{(n+1)}{r_M^{n+2}} Q_{mn}^{(4)} \iint_{S_M \text{ portions}} Y_{nm}(\theta, \varphi) dS \end{aligned} \quad (10)$$

Where \mathbf{n} is the unit outgoing normal of S_M , and \mathbf{Flux}_{nm} corresponds to the sum of the fluxes through the sensor coils.

Table 1 shows some results related to the validation of the z-dipole and z-quadrupole source identifications. These sources are centered and their effects on the three sensors are measured one after the other. In all cases, the consistent results validate the Q_{10} and Q_{20} theoretical values. Thus, when the source is composed of a z-dipole, the result from the Q_{20} sensor measurement is very small. As with the standard sensor, the proposed solution exhibits good filtering of the second order. This filtering capability is less significant for the z-quadrupole case. Indeed, current intensities are close to the sensitivity limits of the oscilloscope, so the accuracy is reduced [5].

	z-dipole source (mA.m ²)		z-quadrupole source (mA.m ³)	
	Calculated	Measured	Calculated	Measured
A ₁₀ sensor	7.854	7.955	/	-0.025
Standard sensor	7.854	7.854	/	0.030
A ₂₀ sensor	/	9.2·10 ⁻⁴	0.732	0.753

TABLE 1. IDENTIFICATION RESULTS WITH TWO DIFFERENT SOURCES PLACED AT THE CENTER

It should be noted in Table I that the result of the calibration using the z-dipole is fairly good, with only 1.3% error.

Another approach, using a few coils with a simple geometry are considered, the identification is performed by rotating these coils around the device. The measured fluxes in different positions are combined and the equivalent multipolar terms are determined by a simpler measurement approach. The Fig.5 illustrates the prototype.

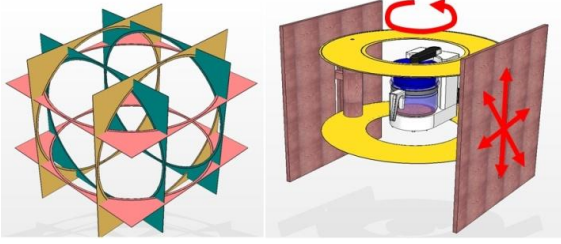


Fig.5 – The new system to identify the terms of the multipolar expansion [5].

IV. COMPUTING THE MUTUAL INDUCTANCE

A. Mutual inductance

Using the equivalent radiated field source model, we can determine the coupling between two equivalent sources through the computation of the mutual inductance. The Fig.6 illustrates the configurations regarding the representation of two radiating sources (Models 1 and 2).

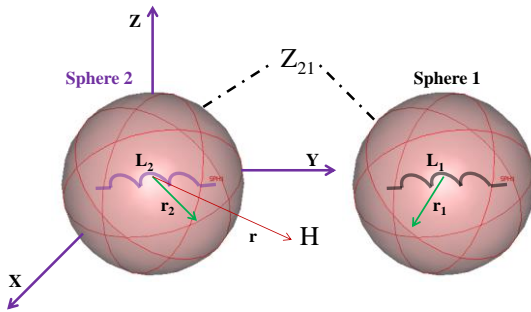


Fig.6 – Representation of two radiating sources.

The computation of the mutual impedance between source 1 and source 2 can be expressed in terms of the electrical field \mathbf{E} and magnetic field \mathbf{H} for each source, by [4]:

$$Z_{12} = -\frac{1}{i_1 i_2} \oint_{\Sigma_1} (\vec{\mathbf{E}}_1 \times \vec{\mathbf{H}}_2 - \vec{\mathbf{E}}_2 \times \vec{\mathbf{H}}_1) \quad (11)$$

When the spheres which contain each of the sources don't intersect, the mutual impedance can be expressed according to the coefficients of the multipolar expansion [4]:

$$Z_{12} = \frac{1}{i_1 i_2} \frac{1}{k^2} \sqrt{\frac{\epsilon_0}{\mu_0}} \sum_{n=1}^{N_{max}} \sum_{m=-n}^n (-1)^m ({}_1 Q_{n,-m}^{(4)} * {}_2 Q_{nm}^{(4)}) \quad (12)$$

The expression of the mutual inductance is:

$$M_{12} = \frac{1}{j \omega i_1 i_2} \frac{1}{k^2} \sqrt{\frac{\epsilon_0}{\mu_0}} \sum_{n=1}^{N_{max}} \sum_{m=-n}^n (-1)^m ({}_1 Q_{n,-m}^{(4)} * {}_2 Q_{nm}^{(4)}) \quad (13)$$

In the expression (12) and (13), i_1 and i_2 are respectively the current circulate in the source 1 and 2, k are phase constant.

The coefficients associated to the magnetic transverse modes of the multipolar expansion of sources 1 and 2 must be expressed in the same reference: a translation is required for example the coefficients of the source 2 can be expressed in the reference of the source 1.

B. Translation and rotation of the coefficients Q_{nm}

The rotation of the coefficients Q_{nm} is obtained by applying the Euler angle reference formula. It should be mentioned that only two angles are necessary because of the spherical symmetry. The details of the methodology for determining the rotation matrices for complex or real coefficients Q_{nm} are presented in [7]-[9].

The translation is based on the « Addition Theorem for Vector Spherical Harmonics » [8].

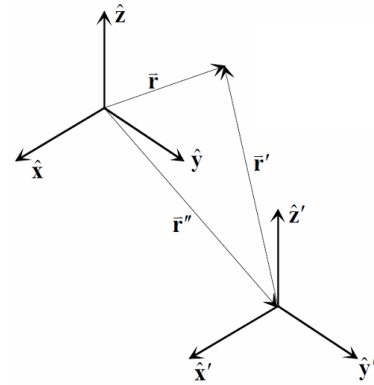


Fig.7 – Translation of a spherical basis

The addition theorem links the harmonics evaluated on r to those evaluated on r' , where r is measured from the origin of the second spherical basis, whose axes are parallel to the first. The origin of the second spherical basis is linked to the first by r'' . These 3 vectors are connected by the relation $r = r' + r''$.

The expression of the translate coefficients Q_{nm} are:

$$Q_{n'm'} = \sum_{n=1}^{\infty} \sum_{m=-n}^n Q_{1mn} A_{n',m',n,m} \quad (14)$$

The coefficient $A_{n',m',n,m}$ computation involves the Wigner 3j symbol according to quantum mechanics [9].

V. VALIDATION

To validate the method of computing the mutual inductance between two equivalent radiated field of the components, the analytical result was compared to the numerical result computed by Flux3D® [10]. For this proposal, two similar loops configuration were considered, C_1 and C_2 . This is a simple case, which, objective is to validate this method in the case of a filter, for two coils.

The results obtained through experimental measurements were led to be presented in a future paper.

A. First case

We consider two loops, C_1 and C_2 with a radius of 10 cm, separated by r , both located on the Oz -axis as shown in the Fig.8. The minimum sphere of validity is the sphere which surface includes the source. In our case the radius of the sphere was assumed equal to the radius loop.

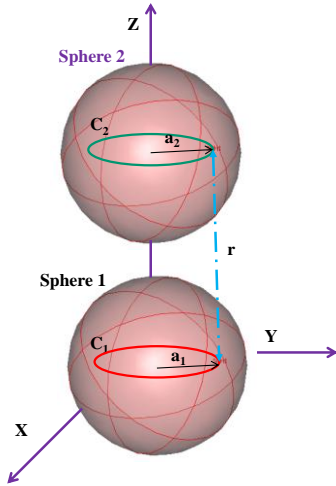


Fig.8 – Two similar coils placed on the z axis

In this case, the method of computing the mutual inductance in flux3D® is based on the computation of the flux through the surface of one of the two loops.

We have computed the mutual inductance between the loops, according to the distance r using the method of spherical harmonics for $n=3$ and $n=5$, and on the simulation of the flux through the surface of one of the

two loops. The result is compared with those computed directly by Flux3D®. The comparison between the results is shown in the Fig.9.

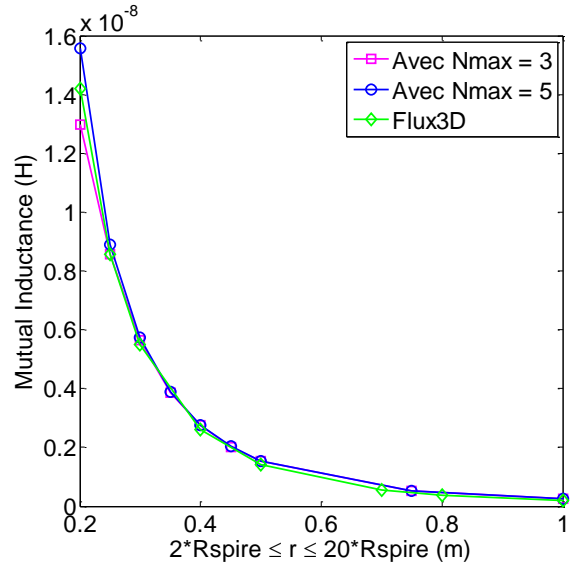


Fig.9 – The comparison between spherical harmonics mutual inductance result and Flux3D® up to the near-field distance limit at 200MHz (1m)

Using the equivalent models of each loop to compute the mutual inductance, there must be no intersection between the spheres that include the source for which of the mutual inductance that will be computed, which has a minimum distance of $(R_{coil1} + R_{coil2}) = 0.2m$ between their centers.

As shown in Fig.9, the results between the method using a truncated multipolar expansion and the numerical method in Flux3D® are comparable.

To compute the mutual inductance for a small distance between the two loops, the number of terms required to describe the complexity of the source increases. For that reason, at distance of $r=0.2m$ the error is greater for $n=3$ than $n=5$ as show in the Fig.10.

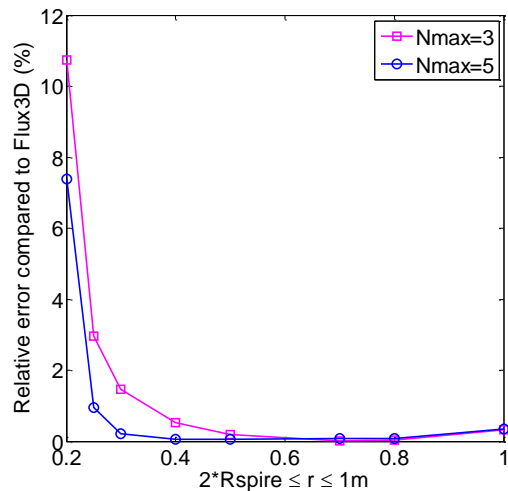


Fig.10 – The relative error compared to Flux3D®

B. Second case

In the second case the numerical method is validated when the theorem to rotate the coefficients Q_{2nm} of the loop C_2 is applied. A rotation of 45° around the y axis corresponds to the 2nd Euler angle as shown in Fig.11

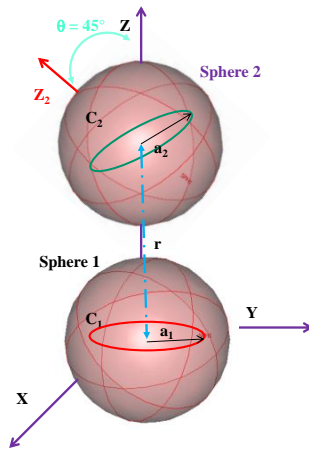


Fig.11 – Two similar coils in oz axis where the coil C_2 is rotate of 45° than the the coil C_1 .

To compute the mutual inductance between the two loops, in the spherical basis of the loop C_1 , it was necessary to rotate the coefficients Q_{2nm} of the loop C_2 before translating them to the spherical basis of loop C_1 . The comparison results of the spherical harmonics method and Flux3D® are represented in Fig.12.

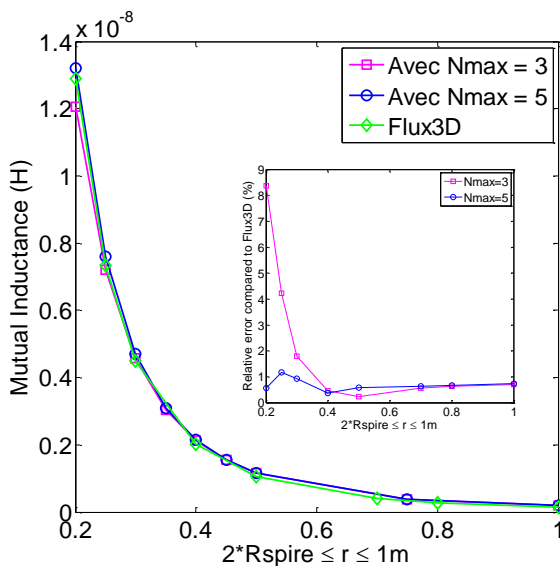


Fig.12 – The comparison between numerical and spherical harmonics results of mutual inductance

The results of the mutual inductance between the two coils are similar to the previous case, at $r=0.2m$, where the error is greater for $n=3$ than $n=5$.

VI. CONCLUSION

This method allows us to create, at first, the equivalent sources which represent the radiated field component using the multipolar expansion. The equivalent sources

will then be used to compute the coupling between them, which was represented by a mutual inductance as a function of the distance that separates them.

Although some simple configurations were used to validate the proposed methodology, some not canonical structures been planned to be evaluated by the authors in the near future. Moreover, other kind of multipolar expansions, like the cylindrical one can be more suitable for modeling components such as tracks or cables, and it will also be considered. For example, in the case of the coupling between a track and a component, the spherical harmonic of the equivalent models of components radiated field is not very adequate and other one should be used.

The method proposed could be helpful when coupled with the PEEC method in the evaluation of equivalent circuit of power electronics devices (R-L-M-C). This will allow considerable gain in memory space concerning the full model configuration used in EMC filter numerical simulations.

The use of experimental results was based on the flux method measuring by large coils placed around the system. It allows a “spatial integration” to reduce the effect of the sensor position errors, unlike to the punctual measurement method where the sensor of magnetic field moves around the object to measure the field at many points, and can also be stressed as a helpful tool concerning the multipolar expansion coefficient determination.

REFERENCES

- [1] S.Wang, F.C.Lee and W.G.Odendaal, “Controlling the parasitic parameters to improve EMI filter performance”, 2004 IEEE, National science foundation under Award Number EEC-9731677.
- [2] S.Wang, F.C.Lee and W.G.Odendaal, “Cancellation of capacitor parasitic parameters for noise reduction application”, IEEE Transactions on power electronics, Vol.21, No.4, July 2006.
- [3] V.Ardon, O.Chadebec, E. Clavel, J-M. Guichon, E. Vialardi V. “EMC Modeling of an Industrial Variable Speed Drive with an Adapted PEEC Method”, COMPUMAG, Florianopolis, Brazil, 22-26 Nov 2009.
- [4] Billy C.Brock « Using vector spherical harmonics to compute antenna mutual impedance from measured or computed fields », SANDIA Report, April 2001
- [5] B. Vincent, O. Chadebec, J.-L. Schanen, K. Berger, « Loop antennas for Near Field Multipolar Expansion Identification: First experimental Validations », to be published in ICONIC 2009 – Special Issue of IEEE Transactions on Instrumentation and Measurement.
- [6] Standard CISPR 16-1, part P, 2002, pp.230-237 and 396-409.
- [7] Miguel A.Blanco, M.Florez and M.bermejo, « Evaluation of the rotation matrices in the basis of the real spherical harmonics », Journal of Molecular Structure : Theochem, Vol.419, Issues 1-3, 8 december 1997, pp. 19-27.
- [8] Advanced Engineering Electromagnetics. Constantine A. Balanis. John Wiley & Sons, 1989, Chapter 10 , pp. 550-552.
- [9] Clebsch-Gordan (C.-G.) Coefficients and '3j' Symbols. A. Messiah, Appendix C.I in Quantum Mechanics, Vol. 2. Amsterdam, Netherlands: North-Holland, pp. 1054-1060, 1962.
- [10] www.cedrat.com